Journal of Molecular Catalysis B: Enzymatic 56 (2009) 61–69

Contents lists available at ScienceDirect

Journal of Molecular Catalysis B: Enzymatic

journal homepage: www.elsevier.com/locate/molcatb

Kinetic analysis for suicide-substrate inactivation of microperoxidase-11: A modified model for bisubstrate enzymes in the presence of reversible inhibitors

K. Nazari [a,b,*], A. Mahmoudi [c], M. Khosraneh [c], Z. Haghighian [b], A.A. Moosavi-Movahedi [a,d]

[a] Institute of Biochemistry and Biophysics, University of Tehran, Tehran, Iran
[b] Research Institute of Petroleum Industry, P.O. Box 18745/4163, Tehran, Iran
[c] Chemistry Department, Karaj Islamic Azad University, Karaj, Iran
[d] International Center of Excellence for Interdisciplinary Sciences, IAU, Tehran, Iran

ARTICLE INFO

Article history:
Received 17 December 2007
Received in revised form 16 April 2008
Accepted 18 April 2008
Available online 26 April 2008

Keywords:
Microperoxidase-11
Suicide inactivation
Inhibition
Heme–peptide
Amino acid

ABSTRACT

Kinetics of microperoxidase-11 (MP-11) as a heme–peptide enzyme model in oxidation reaction of guaiacol (AH) by hydrogen peroxide was studied in the presence of amino acids, taking into account the inactivation of MP-11 during reaction by its suicide substrate, H_2O_2. Reliability of the kinetic equation was evaluated by non-linear mathematical fitting. Fitting of experimental data into a new integrated kinetic relation showed a close match between the kinetic model and the experimental data. Indeed, it was found that the mechanism of suicide-peroxide inactivation of MP-11 in the presence of amino acids is different from MP-11 and/or horseradish peroxidase. In this mechanism, amino acids compete with hydrogen peroxide for the sixth co-ordination position of iron atom in the heme group through a competitive inhibition mechanism.

The proposed model can successfully determine the kinetic parameters including inactivation by hydrogen peroxide as well as the inhibitory rate constants by the amino acid inhibitor.

Kinetic parameters of inactivation including the initial activity of MP-11, α_0, the apparent inactivation rate constant, k_i and the apparent inhibition rate constant for cysteine, k_I were obtained $0.282 \pm 0.006\ min^{-1}$, $0.497 \pm 0.013\ min^{-1}$ and $1.374 \pm 0.007\ min^{-1}$ at $[H_2O_2] = 1.0$ mM, 27 °C, phosphate buffer 5.0 mM, pH 7.0. Results showed that inactivation and inhibition of microperoxidase as a peroxidase model enzyme occurred simultaneously even at low concentrations of hydrogen peroxide (0.4 mM). This kinetic analysis based on the suicide-substrate inactivation of microperoxidase-11, provides a tool and model for studying peroxidase models in the presence of reversible inhibitors. The introduced inhibition procedure can be used in designing activity tunable and specific protected enzyme models in the hidden and reversibly inhibited forms, which do not undergo inactivation.

1. Introduction

Hemoproteins have conquered a prominent position in biotechnology and related research areas. A major problem encountered in studying the intact enzymes is the complexity of correlating changes in the active site with the observed functional changes. Investigations on heme models of peroxidases with well-defined factors allow us to understand the role of the protein in controlling the function of peroxidases [1]. Peroxidases are ferric heme enzymes, which catalyze the oxidation of a variety of substrates by hydrogen peroxide. Microperoxidases as the heme-based biocatalysts and/or biomimics [1–3] for peroxidases obtain from enzymatic cleavage of cytochrome C [4]. Microperoxidases 8, 9 and 11 have been the subject of extensive studies [1,5–7]. There are a few reports on catalase and/or peroxidase activity of hemins with or without axial ligands [8–12]. Comparison of catalytic rates for peroxidase reactions catalyzed by similar derivatives of hemin, mesohemin and deuterohemin does not reveal a discernable trend. Oxidation of tri-*tert*-butylphenol by *m*-chloroperbenzoic acid catalyzed by hemin and mesohemin alkylimidazole derivatives is reported [13]. Mesohemin-based complexes indicate higher catalytic activity in comparison to their hemin analogues considering that the rate-determining step to be formation of compound I. Furthermore, for the peroxidase-type oxidation reactions of guaiacol, it has been shown that the catalytic rates followed the order hemin > mesohemin > deuterohemin [14]. It has been previously

Abbreviations: MP, microperoxidase; HRP, horseradish peroxidase; AH, hydrogen donor; A, absorbance; C-I, compound I; C-II, compound II; Cys, cysteine; His, histidine; Tyr, tyrosine; ABTS, 2,2′-azino(bis(3-ethylbenzothiazoline-6-sulfonic acid)).

* Corresponding author at: Institute of Biochemistry and Biophysics, University of Tehran, Tehran, Iran. Tel.: +98 21 44438526; fax: +98 21 55932428.
E-mail address: nazarikh@ripi.ir (K. Nazari).

1381-1177/$ – see front matter © 2008 Elsevier B.V. All rights reserved.
doi:10.1016/j.molcatb.2008.04.008

shown that catalytic activities of the hemin–peptide complexes do not exceed those of the unsubstituted hemins. The observed dynamic ligand switch between histidine and water may be a possible explanation for the fact that there is no obvious enhancement of the catalytic activity of the hemins–peptide complexes compared to the unsubstituted hemins. This suggests that co-ordination of the histidine ligand protects the iron center from bleaching (decomposition), in agreement with the hypothesis that the primary role of the proximal histidine ligand in peroxidases is stabilization of the $Fe^{(IV)}$=O center (compound I/II) while the distal histidine plays a crucial role in H_2O_2 activation [15–17]. Comparison of peroxidase activities of hemin and microperoxidase-11 (MP-11) in molecular solvents and imidazolium-based ionic liquids has also been reported, previously [18]. High-valent intermediates of MP-8 with hydrogen peroxide and the models for compounds 0, I and II of horseradish peroxidase are presented, previously [19]. The peroxidatic activity of the heme octapeptide (MP-8), has been studied under conditions where formation of compound I was rate limiting [20]. The active form of the substrate was supposed to be hydroperoxide anion, HO_2^-, and an extrapolated second-order rate constant is introduced for the reaction of aquoMP-8 with HO_2^- of $3.7 \times 10^8\ M^{-1}\ s^{-1}$, which is close to the second-order rate constants reported for reaction of the peroxidase with H_2O_2. Indeed, it is believed that the peroxidase enzymes activate H_2O_2 under physiological conditions through a pH-independent, H^+-coupled binding of the required $H_2O_2^-$. The peroxidase activity of MP-8 can be increased more than tenfold in the presence of the guanidinium ion, which is ascribed to formation of the ion-pair $GuaH^+HO_2^-$; this confirms the important role of the invariant distal arginine in the enzymes. A theoretical model consisting of a microscopic kinetic analysis based on the half-life ($t_{1/2}$) of enzyme depletion is described for monosubstrate enzymes by Waley [21–23]. Mechanism-based inactivation of peroxidases by hydrogen peroxide has been well known [24]. The kinetic models for suicide-peroxide inactivation of catalase (as a monosubstrate hemoenzyme) [25], horseradish peroxidase (as a bisubstrate hemoenzyme) [26] and microperoxidase-11 (as a peroxidase model enzyme) [27] were introduced, previously. In these models, the inactivation process can be easily monitored through the time course (progress curve) of the oxidation reaction of the aromatic hydrogen donor substrate [26,28]. The main feature of this study was the presentation of the kinetic equations and indicating the validity and reliability of the kinetic model. The recent report on the kinetics of suicide-peroxide inactivation of microperoxidase-11 revealed that it is similar to the inactivation model of horseradish peroxidase [28].

Oxidative species (mostly radicals) attack a variety of cellular constituents, but proteins are well known to be especially sensitive, with the most susceptible amino acids such as methionine, cysteine, tryptophan, tyrosine and histidine [29,30]. Although hydrogen peroxide is an essential substrate in the catalytic cycle of peroxidase and peroxidase model enzymes like microperoxidases, at higher concentrations it damages the porphyrin ring through the suicide-peroxide inactivation mechanism [27]. The main structural feature of MP-11 is that, similar to most peroxidases, the fifth co-ordination position in the heme is occupied by the imidazole group of His_{18}. In neutral pH, the sixth position is occupied by a weakly bound water molecule, which can be easily replaced by the peroxide substrate.

Amino acids as osmolytes (at high concentrations) can stabilize the protein structure [31,32]. The destabilizing effects of amino acids on the protein structure are also reported elsewhere [29,33]. In contrast to the HRP, easily accessible sixth co-ordination position of the heme iron (peroxide substrate binding site) in microperoxidase and peroxidase biomimetic models, suffers a restriction on the generation of potent enzyme models due to the possible inhibition, tight binding and blocking effects of the present binding agents. Such effectors expected to cause deactivation of peroxidatic activity of the model biocatalysts, which can be monitored by the ligand binding, inhibition and activity measurements.

In the present work MP-11 is selected to evaluate the role of heme active site of peroxidase upon interaction with typical amino acids (Cys, His and Tyr). The advantage of using MP-11 is that MP-11 shows better water solubility, lower tendency to aggregate/dimerize, and a spatial conformation, determined by the polypeptide chain, that resembles in true heme proteins [5]. Indeed, this work discusses the effect of amino acids on the peroxidatic activity, long-term stability, thermostability and suicide inactivation of MP-11 in the presence of its suicide substrate, H_2O_2.

2. Experimental

2.1. Materials

Microperoxidase (sodium salt) and 2,2′-azino(bis(3-ethylbenzothiazoline-6-sulfonic acid)) (ABTS) diammonium salt were obtained from Sigma. Guaiacol (*ortho*-methoxyphenol), L-histidine, L-tyrosine and L-cysteine, $Na_2HPO_4{\cdot}2H_2O$ and hydrogen peroxide 30% (V/V) were obtained from Merck. Phosphate buffer 5.0 mM, as the solvent system for the all other reagents was prepared in CO_2-free deionized water (Barnstead NANOpure D4742 deionizer, electrical resistance = 18.3 MΩ).

2.2. Methods

Absorbance changes and electronic spectra were recorded using a Varian spectrophotometer model Cary 50 equipped with fiber optic dip probe accessory and a xenon light source. The fiber optic probe provides the data recording at the time of mixing in the reaction vessel. The ionic strength and pH of the solutions were kept constant by using a 5.0 mM phosphate buffer. Temperature of the reaction solution in the jacketed laboratory reactor (4 mL) was adjusted at 25 °C (±0.1) using a Lauda water circulating thermobath equipped with an external temperature sensor.

Difference Spectrophotometric titration experiments of MP-11 with amino acids (His, Tyr and Cys) were carried out at 404 nm, 25 °C in phosphate buffer 5.0 mM, pH 7.0. Specific activity of MP-11 was determined spectrophotometrically in a 1-min reaction time course using 2,2′-azino(bis(3-ethylbenzothiazoline-6-sulfonic acid)) (ABTS) [34].

ABTS as a chromophoric reducing substrate is very convenient for monitoring peroxidase activity. The biocatalytic reaction can easily be monitored by following formation of the $ABTS^{+\bullet}$ radical at the maximum absorption wavelength, λ_{max} = 414 nm and peroxidase activity of MP-11 was estimated using the known relevant relation using an extinction coefficient of ε_{414} = 36.0 $mM^{-1}\ cm^{-1}$ for the oxidized ABTS [34].

The peroxidase specific activity of MP-11 was obtained 72.0 U/mg at 25 °C, pH 7.0 (phosphate buffer 5.0 mM). One unit (U) is the amount of MP-11 that catalyzes the oxidation of 1 μmol of ABTS per minute. Specific activity (U/mg) is the number of MP-11 units per mL divided by the concentration of microperoxidase in mg/mL.

MP-11 concentration was determined at pH 7.0 using an extinction coefficient of 176 $mM^{-1}\ cm^{-1}$ at 395 nm [6] and concentration of hydrogen peroxide was estimated by measuring absorbance of the solution using ε_{240} = 43.6 $cm^{-1}\ M^{-1}$ [35]. In all calculations, a molecular weight of 1861.9 was used for MP-11.

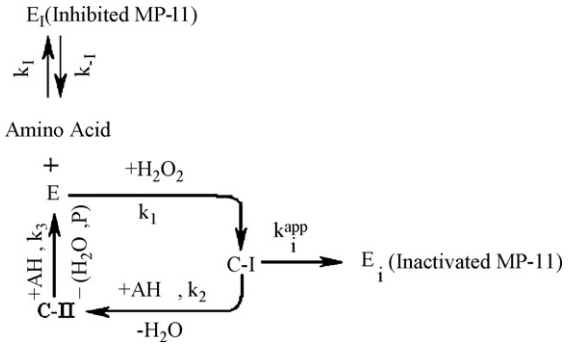

Scheme 1.

The same spectrophotometer in the kinetic mode was used to recording the progress curves of the inactivation process. Suicide-peroxide inactivation of MP-11 was monitored at 470 nm (λ_{max} for the product of the guaiacol oxidation reaction, $\varepsilon_{470} = 26.6\ cm^{-1}\ mM^{-1}$) by difference spectrophotometry. The details of the procedure of measuring the product concentration, the rate of reaction, and determination of the progress curves have been described previously [27].

Before start of the reaction, complexes of MP-11 and amino acids with molar ratios of 0.2, 0.5, 1 and 10 of [amino acid]/[MP-11] were prepared. Progress curves were obtained by following absorbance of the reaction mixture at 470 nm in an appropriate time course of about 30 min. A 30-s period was kept as delay time for addition of H_2O_2 to the solution system of MP-11/amino acid/AH, stirring and making the mixture homogeneous. The unreacted part of AH was obtained from the recorded absorbance data and suitable relations [27]. Each experiment was repeated three times and standard deviations were estimated for the obtained results.

3. Results and discussion

In the presence of H_2O_2 [36], microperoxidases form reactive intermediate like peroxidase compound I, which can oxidize aromatic substrates, effectively [7]. This stable intermediate may undergo suicide inactivation in the presence of hydrogen peroxide (≥0.4 mM). Indeed, it has been shown that in the presence of high concentrations of peroxide, in addition to the major catalytic pathways, microperoxidases and peroxidases can also enter into the "suicide-substrate inactivation" pathway [26,29,37–40]. The inactivation process starts by the reaction of excess H_2O_2 with compound I. The product of the inactivation process (P-670) is a catalytically inactive form of peroxidase (E_i in Scheme 1) [26,41–43]. This inactive form indicates a λ_{max} in its electronic spectra at 670 nm. P-670 with a low molar absorptivity is unstable and may convert into the subsequent inactive forms [27].

In the case of peroxidase it is observed that amino acids (His, Tyr and Cys) at low concentrations activate HRP and protect the enzyme against suicide inactivation by H_2O_2 [44]. Interestingly, such behavior was not repeated for the interaction of amino acids with MP-11 and a decrease in the peroxidatic activity of MP-11 was observed. This deactivation can be attributed to the possible bonding of the amino acid on the free sixth position of iron atom in MP-11. As presented further, results show that the deactivation occurs via a competitive inhibition process (see Fig. 3). The simultaneous and concurrent inhibition of MP-11 by the amino acid and its inactivation by the suicide substrate (H_2O_2) is measured through its catalytic reaction cycle (depletion of aromatic substrate) (see Eqs. (5)–(20)). Among the MP-11 active forms (including MP-11, C-I and C-II), compound I as a π-radical cation intermediate shows the maximum potential to oxidize aromatic substrates through the catalytic reaction cycle. However, in the presence of amino acids, MP-11 (E_a in the Scheme 1) can only react with them from the free sixth position:

Scheme 1 shows the catalytic reaction cycle, the inactivation and inhibition pathways for MP-11. According to Scheme 1, three major reactions could be attributed to the reaction system

$$E_a \xrightarrow{(H_2O_2)k_i} E_i \quad (a)$$

$$E_a \xrightarrow{(\text{amino acid})k_I} E_I \quad (b)$$

$$AH \xrightarrow{(H_2O_2, E_a)\alpha} P \quad (c)$$

Reactions a and b are the inactivation and inhibition reactions, respectively. Reaction c (oxidation of guaiacol by peroxide) is the catalyzed reaction, which is also used to monitor the inactivation process. E_a, E_i, E_I, AH, and P denote the whole forms of active enzyme, inactivated enzyme, inhibited enzyme, hydrogen donor (reductant-substrate) and the catalytic reaction product (tetraguaiacol), respectively. Parameters of k_i, k_I and α denote the apparent rate constant of inactivation (reaction a), apparent rate constant of inhibition (reaction b) and the apparent catalytic rate constant of the oxidation reaction (reaction c), respectively. In the catalytic reaction cycle, the active enzyme species are free active enzyme (E_a), C-I and C-II. The rate constants of formation of C-I, C-II and E_a are extremely large [45] compared with the k_i and k_I values. According to the mechanism C-I may enter into the inactivation pathway and E_a undergoes inhibition by the amino acid (see Scheme 1). The following conditions are recommended for the simultaneous advancement of the three reactions (a, b and c):

(1) Higher concentration of hydrogen peroxide with respect to the concentration of hydrogen donor (AH).
(2) Low concentration of hydrogen donor ("benign substrate", a substrate that does not damage the enzyme); so the donor substrate does not saturate the enzyme (according to the initial linear part of the Michaelis–Menten plot).
(3) Concentration of amino acids should be in the range of catalytic concentration of MP-11 so that the molar ratio of [amino acid]/[MP-11] was 0.2–10.0 and the amino acid does not act as osmolytes at this low concentration range.

The reaction c is essentially first-order in relation to the hydrogen donor and similar to HRP [27] and MP-11 [28] alone, a linear dependence on the initial velocity of the reaction at low concentrations of AH was observed (data not shown) [27]. As a result, the rate of reactions a and b seem to be proportional to the active enzyme concentration. Using a steady-state approximation, it is possible to derive the differential and integrated kinetic equations. In principle, by monitoring AH concentration in the catalytic reaction cycle; one can estimate the extent of decrease in the level of active forms of the enzyme (due to the suicide inactivation process).

Previously, the corresponding kinetic equations for suicide-peroxide inactivation of catalase [25], horseradish peroxidase [26] and micrperoxidase-11 [27] have been reported. Also protective effect of Ni^{2+} ion on the suicide inactivation of HRP [46] and a model for simultaneous deactivation/inactivation of HRP in the presence of sodium dodecyl sulfate and hydrogen peroxide were presented recently [35].

Fig. 1 illustrates the effect of amino acids on the activity of MP-11. It can be observed that increasing the mole ratio of amino acid/MP-11 is associated with a decrease in the peroxidatic activity. Furthermore, cysteine has a more distinct lowering effect on the catalytic activity of MP-11. It can be expected that amino acids with their strong electron donor groups (like amine, sulfur, carboxyl and hydroxyl) are able to bind on the free position of iron atom in

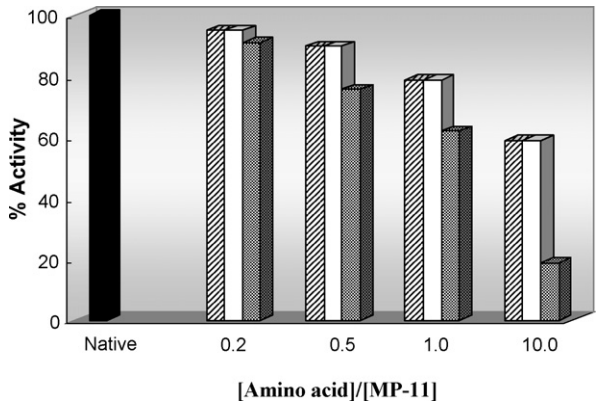

Fig. 1. Dependence of peroxidatic activity of MP-11 with the type and mole ratio of [amino acid]/[MP-11] at suicide conditions, $[H_2O_2] = 1.0$ mM, [AH] = 0.4 mM at 27 °C, pH 7.0 phosphate buffer 5.0 mM. (■) MP-11 native; (▨), His; (□) Tyr; (▩) Cys.

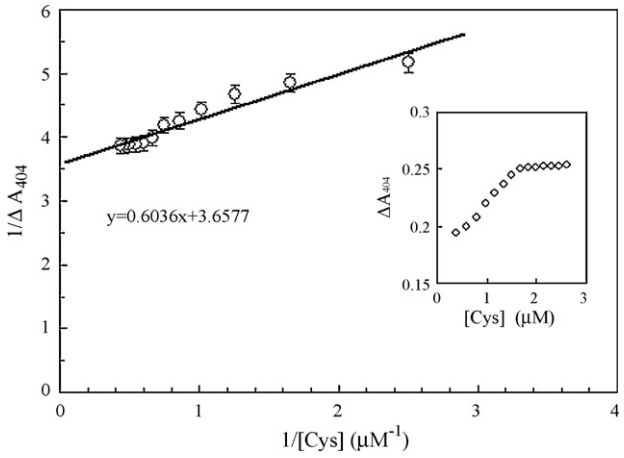

Fig. 2. Double-reciprocal plot based on Eq. (1) for binding of Cys on MP-11. The data are obtained from the spectrophotometric titration of MP-11 with Cys (inset of the figure). Inset: titration of MP-11 solution (1.0 μM) with a cysteine solution (14.2 μM) in phosphate buffer 5.0 mM, pH 7.0 and temperature of 27 °C. The points show the absorbance changes after additions of Cys corresponding to [Cys]/[MP-11] ratios from 0.2:1.0 to 2.5:1.0. Five minutes was considered for each addition to equilibrate the reaction mixture.

the center of porphyrin ring (E_a in Scheme 1). For the amino acids under study, p*K*a values are in the range of 6.7–7.1, 8.8–9.1, 9.7–10.1 for His, Cys and Tyr, respectively [47]. Generally, the amine group of the amino acids is protonated at neutral pH but this group can easily bind to the transition metal ions by a subsequent deprotonation [48]. Thus, despite of their positive net charge at pH 7.0, Tyr and Cys are expected to bind to the iron via the amine group.

It means the amino acids might compete with hydrogen peroxide for the sixth position of the iron atom of MP-11. Therefore, the equilibrium constants for formation of MP-11/amino acid complexes were estimated by spectrophotometric titration of MP-11 by the amino acids (His, Tyr and Cys) in phosphate buffer 5.0 mM at 25 °C. The experimental data were analyzed considering a simple equilibrium $M + L \rightleftarrows ML$. The equilibrium constant (K_d) and molar absorptivity (ε) of the formed complexes were estimated by fitting the experimental data into the double-reciprocal plot namely Benesi–Hildebrand relation [49–51]:

$$\frac{1}{\Delta A} = \left(\frac{K_d}{\Delta A_\infty}\right) \times \frac{1}{[L]} + \left(\frac{1}{\Delta A_\infty}\right) \quad (1)$$

$$\Delta A_\infty = \varepsilon b[\text{MP-11}] \quad (2)$$

where K_d is the dissociation constant of the MP-11–ligand complex, ΔA is the observed difference absorbance change at the wavelength of maximum absorbance (λ_{max}) 404 nm, ΔA_∞ is the maximum absorbance change and [*L*] represents the ligand concentration. ε is the molar absorptivity (extinction coefficient) of the complex and *b* is the light path-length. Eq. (1) indicates linear changes of $1/\Delta A$ versus $1/[L]$ with *Y*-intercept of $1/\Delta A_\infty$ and slope of $K_d/\Delta A_\infty$. Thus, K_d could be determined from the slope of the plot by a simple linear regression. Fig. 2 illustrates such plot for the interaction of Cys with MP-11. Fig. 2:inset shows the corresponding profile for spectrophotometric titration of MP-11 with Cys in phosphate buffer solution 5.0 mM, pH 7.0 and temperature of 25 °C.

At concentrations below 25 μM, the aggregation (dimerization) of MP-11 can be neglected [12]. K_d and ε_{404} values for the three amino acids/MP-11 complexes are shown in Table 1. According to the table, Cys indicates a binding constant (association constant), $K_a = 6.046 \times 10^6\ M^{-1}$ which reflects the high affinity of this inhibitor for the sixth position of iron center of MP-11.

In the next step, in order to examine the existence and the type of probable inhibiting effects of the amino acids, Michaelis–Menten model was checked on the kinetics of MP-11 using hydrogen peroxide as the varying substrate and cysteine as the inhibitor. In reversible inhibition, enzyme activity can be recovered when the inhibitor is removed [24]. Once the type of inhibition has been established, it is possible to determine the inhibition constant, K_I.

Regarding the Lineweaver–Burk plot drawbacks [52,53] it is better to use the other models like Dixon plot [54]:

$$\frac{1}{V} = \left\{\left(\frac{K_m}{V_{max}}[S]\right) \times \frac{[I]}{K_I}\right\} + \left(\frac{K_m}{V_{max}}[S]\right) + \left(\frac{1}{V_{max}}\right) \quad (3)$$

at $[I] = -K_I$ the $1/V$ function would be independent of [S] (at constant amount of the enzyme), since at such condition Eq. (3) leads to:

$$\frac{1}{V} = \frac{1}{V_{max}} \quad (4)$$

According to Eq. (3) and at fixed [S], a plot of $1/V$ against [I] (the Dixon plot) is linear. Thus, in the presence of reversible competitive inhibitor, the inhibitory constant (K_I) can be determined from the intersection point where $[I] = -K_I$.

As Fig. 3 confirms, a reversible competitive inhibition was observed for the interaction of cysteine with MP-11. The values of V_{max}, K_I and K_m were obtained 0.197 mM min^{-1}, 3.71×10^{-4} mM and 0.352 mM, respectively. Furthermore, using rapid-equilibrium approximation for the kinetics of binding of reversible inhibitor ($K_I = k_{-I}/k_I$) and knowing K_I from the Dixon plot (Fig. 2) and k_I from Table 2 (average value at molar ratios 0.2 and 0.5 of Cys/MP-11), it is possible to estimate the value of k_{-I}. Thus, over the molar ratio of 0–0.5 for Cys/MP-11, value of k_{-I} was obtained $1.23 \times 10^{-3}\ min^{-1}$. It shows that at the above molar ratio of Cys/MP-11, there is a reversible competitive inhibition on the active site, which allows the dead-end irreversible inactivation of MP-11 through the reaction a.

As described above, MP-11 with one free position at the sixth position and a His bound at the fifth position, shows a competitive inhibition effect of amino acid in relation to the suicide substrate, H_2O_2. At low concentrations of hydrogen peroxide (typically lower

Table 1
Dissociation constants (K_d) for binding of amino acids on the sixth position of the Fe(III) center of MP-11 obtained from spectrophotometric titration of MP-11 with the amino acids using Eq. (1)

Complex	K_d ($\times 10^7$ M)	ε_{404} ($\times 10^{-5}\ M^{-1}\ cm^{-1}$)
His/MP-11	2.874 ± 0.132	3.52 ± 0.15
Tyr/MP-11	4.922 ± 0.152	2.53 ± 0.12
Cys/MP-11	1.654 ± 0.078	2.73 ± 0.13

Experimental conditions: phosphate buffer 5.0 mM, pH 7.0, $T = 25$ °C

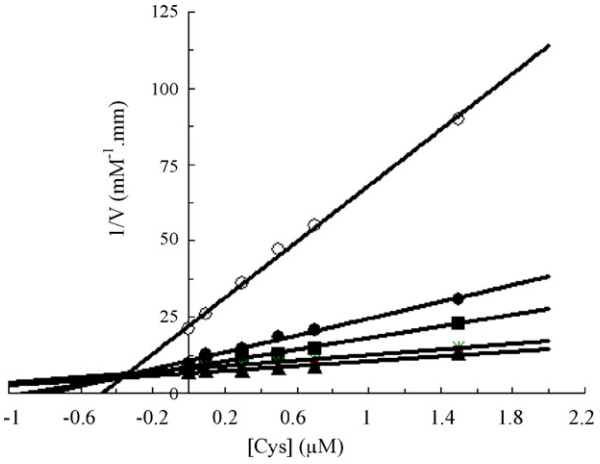

Fig. 3. Dixon plot as the variation $1/V$ vs. [Cys] in the presence of various concentration of hydrogen peroxide based on Eq. (3). Before the experiments, solutions of microperoxidase-11 (1.0 μM) were incubated with various fixed concentrations of inhibitor (cysteine) at pH 7.0 phosphate buffer 5.0 mM, T = 27 °C and [guaiacol] = 0.4 mM. (○) [H_2O_2] = 0.1 mM; (●) [H_2O_2] = 0.3 mM; (■) [H_2O_2] = 0.5 mM; (*) [H_2O_2] = 0.7 mM; (♦) [H_2O_2] = 0.9 mM; (▲) [H_2O_2] = 1.0 mM.

than 0.4 mM) there is no remarkable suicide inactivation effect. At high peroxide concentrations (typically higher than 1 mM), inhibition effect of the amino acid and inactivation effect of H_2O_2 occurred, simultaneously. Since this kind of inhibition by the amino acid is generally reversible and does not damage the enzyme, it can be introduced as a safe storage of the biocatalyst in the reaction mixture containing high concentrations of the suicide substrate. It means this inhibition mechanism can reduce the population of biocatalyst exposed the suicide substrate, since inhibited MP-11 does not undergo suicide inactivation (see Scheme 1).

In order to model the inhibition/inactivation mechanism and according to reactions a, b and c since practically reaction a is an irreversible inactivation, hence, the rate of inactivation can be expressed as

$$-\left(\frac{d\alpha_1}{dt}\right) = k_i^{app}\alpha \tag{5}$$

Reaction b shows the reversible inhibition of the biocatalyst by the amino acid. Therefore, contribution of the inhibition process in lowering the active enzyme level can be expressed as

$$-\left(\frac{d\alpha_2}{dt}\right) = k_I^{app}\alpha \tag{6}$$

$$-\left(\frac{d\alpha}{dt}\right) = -\left[\left(\frac{d\alpha_1}{dt}\right) + \left(\frac{d\alpha_2}{dt}\right)\right] = (k_i^{app}\alpha) + (k_I^{app}\alpha) = (k_i^{app} + k_I^{app})\alpha \tag{7}$$

$$(k_i^{app} + k_I^{app}) = k_{iI}^{app}, \qquad -\left(\frac{d\alpha}{dt}\right) = k_{iI}^{app}\alpha \tag{8}$$

where k_I is the apparent inhibition rate constant. Apparent rate constants depend on the other effective parameters. For example, k_i^{app} as the apparent inactivation rate constant depends on peroxide concentration. Also k_I^{app} as the apparent inhibition rate constant clearly depends on the inhibitor (amino acid) concentration.

Confirmation of Eq. (8) was checked by a kinetic analysis using steady-state approximation for the mechanism shown in Scheme 1 (see Appendix A). On this basis, the following equation can be obtained as indicated in Appendix A:

$$-\left(\frac{d\alpha}{dt}\right) = \left\{k_I[I] - k_I - k_1[H_2O_2]\right\}\alpha \tag{9}$$

Eq. (9) is similar to Eq. (8), which reflects the accuracy of the proposed model. As Eq. (9) shows the rate of depletion of enzyme in the presence of both the suicide substrate [H_2O_2] and the inhibitor (amino acid) does not depend on the [H_2O_2], but it depends directly on the inhibitor concentration. Indeed as previously reported, k_i itself is a linear function of peroxide concentration [27].

Comparing Eq. (8) with Eq. (9) gives:

$$k_{iI}^{app} = \left\{k_I[I] - k_I - k_1[H_2O_2]\right\} \tag{10}$$

From Eq. (9) we have the following:

$$-\left(\frac{d\alpha}{dt}\right) = \left\{k_I[I] - k_I\}\alpha - \{k_1[H_2O_2]\right\}\alpha \tag{11}$$

Comparing Eq. (7) with Eq. (11) gives:

$$k_i^{app} = k_1[H_2O_2], \qquad k_I^{app} = k_I[I] - k_I \tag{12}$$

Hence, k_i^{app} is a function of peroxide (suicide substrate) concentration and k_I^{app} is a function of inhibitor concentration.

Now, the rate equations for the three reactions including consumption of substrate, inactivation of MP-11 by peroxide and inhibition of MP-11 by the amino acid can be combined. Integration of Eqs. (5) and (6) result in

$$\alpha_1 = \alpha_0\, e^{(-k_i t)} \tag{13}$$

$$\alpha_2 = \alpha_0\, e^{(-k_I t)} \tag{14}$$

Eqs. (7) and (8) can be rewritten as

$$\alpha = \alpha_1 + \alpha_2 = \alpha_0(e^{-k_i t} + e^{-k_I t}) \tag{15}$$

where α_0 can be defined as the value of α at start time of measurements.

According to the reaction c, the rate of conversion of aromatic substrate (guaiacol) to the product can be written as

$$-\left(\frac{d[AH]}{dt}\right) = \alpha[AH] \tag{16}$$

Evaluation and confirmation of Eq. (16) was rechecked by a kinetic analysis using steady-state approximation for the mechanism shown in Scheme 1 (see Appendix B). On this basis, the

Table 2
Kinetic parameters of α_0, k_i and k_I for simultaneous suicide-peroxide inactivation and amino acid inhibition of microperoxidase-11 at pH 7.0 phosphate buffer 5.0 mM, 27 °C, [H_2O_2] = 1.0 mM, [MP] = 1.0 μM

	MP-11-His complex			MP-11-Cys Complex			MP-11-Tyr Complex		
	α_0	k_i	k_I	α_0	k_i	k_I	α_0	k_i	k_I
Native MP-11	0.258	0.494	0	0.258	0.494	0	0.258	0.494	0
[Amino acid]/[MP-11] = 0.2	0.243	1.035	1.483	0.216	0.751	3.123	0.189	0.498	1.452
[Amino acid]/[MP-11] = 0.5	0.234	1.514	2.181	0.176	0.933	3.511	0.132	0.690	1.791
[Amino acid]/[MP-11] = 1.0	0.231	1.692	3.923	0.131	1.102	4.028	0.129	1.044	3.904
[Amino acid]/[MP-11] = 10.0	0.231	1.744	5.112	0.114	1.044	5.126	0.102	0.978	4.811

Parameters were obtained by fitting of the experimental into Eq. (20) using Excel Solver

following equation can be obtained as indicated in Appendix B:

$$-\frac{d[AH]}{dt} = 2\left(\frac{k_1 k_2}{k_i}\right)[E][AH] \quad (17)$$

Eq. (17) is similar to Eq. (16), which represents a relation for α (Eq. (18)) from the microscopic point of view. As Eq. (17) shows the rate of depletion of AH does not depend on the $[H_2O_2]$ directly. Comparing Eq. (17) with Eq. (16) gives:

$$\alpha = 2\left(\frac{k_1 k_2}{k_i}\right)[E] \quad (18)$$

Clearly, Eq. (18) shows that the enzyme activity (α, apparent catalytic rate constant of the oxidation reaction (reaction c)) depends on the rate constants k_1 and k_2 (responsible for conversion of the AH substrate to the colored product) of the catalytic cycle. Also, the enzyme activity depends inversely on the k_i^{app} of the inactivation reaction (causing to depletion and inactivation of the enzyme catalyst and lowering the active enzyme level).

Now, substitution of α from Eq. (15) into Eq. (16) gives:

$$-\left(\frac{d[AH]}{dt}\right) = \alpha_0(e^{-k_i t} + e^{-k_I t})[AH] \quad (19)$$

After rearrangement and integration, we have the following:

$$[AH]_t = [AH]_0\left\{\mathrm{Exp}\left(\frac{\alpha_0}{k_i}(e^{-k_i t} - 1)\right) \times \mathrm{Exp}\left(\frac{\alpha_0}{k_I}(e^{-k_I t} - 1)\right)\right\} \quad (20)$$

where $[AH]_t$ and $[AH]_0$ are concentrations of AH at time t and at start time of measurements ($t = 0$), respectively. Eq. (20) characterizes an overall progress curve ($[AH]_t$ versus time) which is reflecting simultaneous advancement of three reactions of a, b and c. Reaction c as the biocatalytic reaction is used for monitoring the phenomena and guaiacol (reductant substrate, AH) is selected as the probe which produces a colored product with a maximal absorbance at 470 nm. The first factor $\mathrm{Exp}(\alpha_0/k_i(e^{-k_i t} - 1))$ specifies the contribution of inactivation effects according to the reaction a and the second factor $\mathrm{Exp}(\alpha_0/k_I(e^{-k_I t} - 1))$ represents the contribution of inhibition effects of the amino acid, based on reaction b.

Eq. (20) can be used for the determination of α_0, k_i and k_I in a non-linear regression manner by fitting the experimental data ($[AH]_t$ and t) into the equation. Common computer software such as Excel Solver was used for this purpose. Table 2 indicates the obtained values of kinetic parameters for simultaneous suicide inactivation/inhibition of MP-11.

Fig. 4 shows the various inactivation progress curves of MP-11 in the presence of different amino acids. Details of the experiments are described in the legend of Fig. 4. Excellent coincidence between experimental data (points) and the fitted curve (calculated) based on Eq. (20) was observed as shown in Fig. 4. Fig. 4 illustrates the accuracy of the kinetic model and the Eq. (20) for the simultaneous suicide-peroxide inactivation and competitive inhibition of microperoxidase-11 by the amino acids. Furthermore, Fig. 4 demonstrates that (in contrast to HRP), low concentrations of amino acids (as low-dose effectors) cannot protect microperoxidase against suicide inactivation since in the case of MP-11 alone; consumption of guaiacol is higher than the case of amino acid/MP-11 complexes. The same trend was observed (data not shown) for the other used ratios of [amino acid]/[MP-11] (0.2, 1.0 and 10.0). As it is shown in Table 2, inactivation rate constant, k_i and inhibition rate constant, k_I were increased with increasing molar ratio of amino acid/MP-11 while initial activity of MP-11, α_0, was decreased meaning that MP-11 activity diminishes due to the inactivation and inhibition effects. Fig. 1 and Table 2 illustrates that the extent of inactivation on MP-11/amino acid complexes has the inverse order of α_0 values i.e. α_0 (His) > α_0 (Cys) > α_0 (Tyr). According to Fig. 4, among the microperoxidase/amino acid complexes, MP-11/His complex with higher initial activity is able to catalyze the oxidation reaction in a more extensive manner. On the other side, this specificity (i.e. higher concentrations of active form, E_a) would be associated with higher k_i values in the order of k_i (His) > k_i (Cys) > k_i (Tyr) as shown in Table 2. Interestingly, the order of k_I values is consistent with the strength of donor atom of the amino acid side-chain (S for cysteine, N for histidine and O for tyrosine) as k_I (Cys) > k_I (His) > k_I (Tyr) (see Table 2).

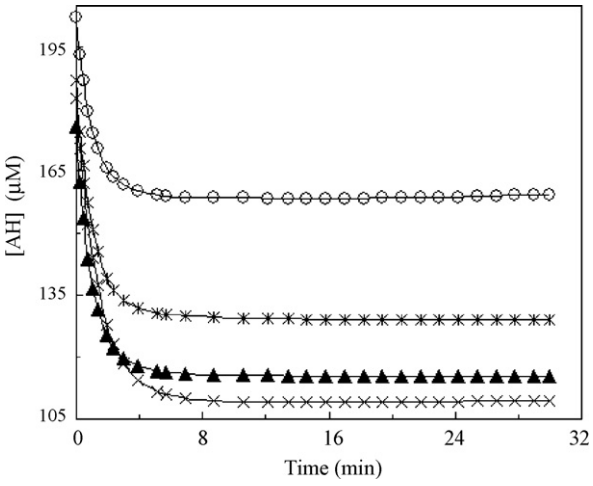

Fig. 4. Progress curves for suicide inactivation of MP-11 by hydrogen peroxide, as the variation of guaiacol concentration vs. reaction time, according to Eq. (20). Inactivation rate constant, k_i and the initial activity of biocatalyst, α_0, were estimated by successive approximation and non-linear fitting of the experimental data into the Eq. (20). Solid lines indicate the calculated curve data using the obtained k_i and α_0 parameters in Eq. (20). Values of the kinetic parameters are shown in Table 2. Each parameter was systematically adjusted to produce best fit curves that gave a minimum value of the sum-of-squares of residuals (SSR, as the differences between observed and calculated values of progress curves, i.e. $SSR = \Sigma(y_{obs.} - y_{calc.})^2$). An Excel Solver program was used for this purpose. A detailed description of the suicide-peroxide inactivation model is given in Refs. [25–28,32]. AH concentration was followed from the absorbance of the reaction mixture at 470 nm using $\varepsilon_{470} = 26.6\ cm^{-1}\ mM^{-1}$ (for details of the calculation procedure see Ref. [27]). Reactions were started by adding hydrogen peroxide (1.0 mM in the reaction mixture) to a solution of AH (200 μM) and MP-11 (1.0 μM) having an initial activity of 0.3 min.$^{-1}$, time course of about 30 min at 27 °C, phosphate buffer 5.0 mM, pH 7.0. All the curves are corresponding with the ratio of [amino acid]/[MP-11] = 0.5, and for the other ratios similar trend was observed, too. (×) Native MP-11; (*) Tyr/MP-11; (○) Cys/MP-11; (▲) His/MP-11.

Furthermore, there are some reports on the stabilizing effects of amino acids on the structural stability of proteins and enzymes. In these cases amino acids as osmolytes and at high concentrations stabilizes the macromolecule structure [31,32]. It is also reported denaturational effects of histidine on the protein structure, which reflects the destabilizing effects of amino acids [29,33].

In order to check the effect of amino acids on the structural stability of MP-11, thermostability experiments were performed at 50 °C and higher ratio of [amino acid]/MP-11, by periodical measuring the peroxidatic activity (guaiacol assay) within about 24 h. The result is shown in Fig. 5, which indicates a fast and probably irreversible inhibition for cysteine that can be attributed to its higher affinity and stronger binding to the iron atom at higher temperatures (50 °C). Thermostability of MP-11 in the presence of His and/or Tyr remains unchanged within this time period, which means amino acids, have no significant structural effects on MP-11 and they only act as the inhibitor. For fine-tuning the effect of cysteine on thermostability of MP-11, experiments were repeated over a range up to [Cys]/[MP-11] = 1.5

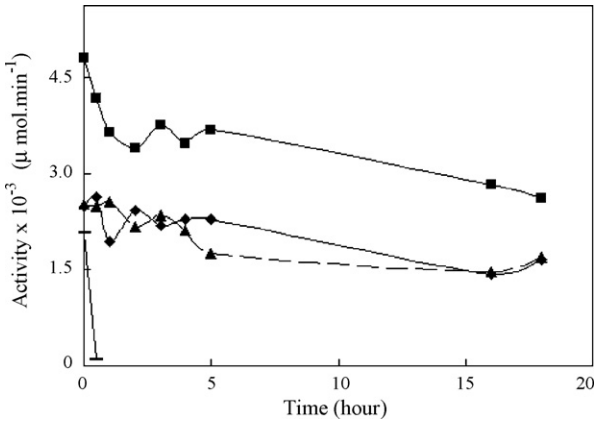

Fig. 5. Thermostability of MP-11 vs. time in the presence of amino acids (molar ratio of amino acid/MP-11 = 10.0). Activity measurements were performed at pH 7.0, 50 °C, [AH] = 0.4 mM, [H_2O_2] = 1.0 mM, [MP-11] = 1.0 μM. Enzyme activity = rate of reaction (μmol L^{-1} min^{-1}) × volume of reaction mixture (L). (■) Native MP-11; (♦) His/MP-11; (▲) Tyr/MP-11; (–) Cys/MP-11.

as shown in Fig. 6. The figure shows that cysteine at molar ratio of [Cys]/[MP-11] = 1.5 completely inhibits peroxidatic activity of MP-11. Another interesting aspect of Fig. 6 is that it is possible to control and tune the activity of MP-11 by using a desirable amount of cysteine. For example using a molar ratio of [Cys]/[MP-11] = 1.0, peroxidatic activity of MP-11 can be controlled around 1.8×10^{-3} μM min^{-1}.

It must be mentioned that Cys alone can also act as a reducing agent in the conversion of Fe(III) (catalytically active form) to Fe(II) (catalytically inactive form) in microperoxidase. But in the presence of hydrogen peroxide (referred to as activation mechanism of hydrogen peroxide) formation of CI (a π-radical cation of Fe(IV) = O species) with a very large rate constant (~10^7 s^{-1}) is expected to be the main reaction and probably there is no chance for Cys to reduce the ferric center. But at high temperatures (50 °C; see Fig. 5) Cys perhaps shows such a behavior since a strong and nearly irreversible inhibition observed just for this amino acid and not for His and Tyr. Furthermore, to check substrate behavior for cysteine and tyrosine [54], cysteine was used as the hydrogen donor substrate (instead of guaiacol) in the assay. However, spectrophotometry and HPLC methods detected no reaction product (data not shown).

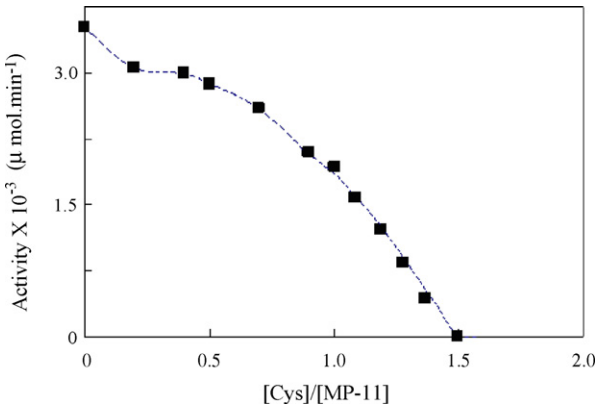

Fig. 6. Activity vs. [Cys]/[MP] ratio at pH 7.0 phosphate buffer 5.0 mM, 50 °C, [AH] = 0.4 mM, [H_2O_2] = 1.0 mM, [MP] = 1.0 μM. Measurements were done after 5.0 min to equilibrate the system. Enzyme activity = rate of reaction (μmol L^{-1} min^{-1}) × volume of reaction mixture (L).

Long-term stability experiments as the variation of catalytic activity versus time (up to about 8 weeks) were also confirmed deactivation of MP-11 by the amino acids (data not shown), in which activity of native MP-11 was considerably greater than the MP-11/amino acid complexes.

Such controllable activity of MP-11 can be used in designing specific protected biocatalysts in the form of hidden and reversibly inhibited, which does not enter into the inactivation pathway. Also such a protection procedure plus media engineering can be used for preparing specific biosensors and nano-devices. This is the subject of current research plan in this laboratory including protection of MP-11 against the suicide substrate (hydrogen peroxide), manufacturing and application of nanosilica immobilized MP-11 biosensors for detection of phenolic compounds.

4. Conclusions

Kinetics of simultaneous inhibition/inactivation of microperoxidase-11 (MP-11) in oxidation reaction of guaiacol (AH) by hydrogen peroxide showed the major part of suicide-peroxide inactivation and the reversible competitive inhibition by the typical amino acids. The proposed model can successfully determine the kinetic parameters including inactivation by hydrogen peroxide as well as the inhibitory rate constants by the amino acid inhibitor. General aspects of the model are as follows:

(1) The reaction is first-order in relation to the aromatic hydrogen donor, AH.
(2) High ratio of suicide substrate to the aromatic benign substrate, [H_2O_2] ≫ [AH].
(3) Preferentially, concentration of the amino acid as the low-dose effector, might be around the catalytic concentration of MP-11, typically, molar ratio of amino acid/MP-11~0.2–10.0.
(4) The introduced inhibition procedure can be used in designing activity tunable and specific protected enzyme models in the hidden and reversibly inhibited forms, which do not undergo inactivation.
(5) At high peroxide concentrations (typically higher than 1 mM), in which simultaneous reversible inhibition by the amino acid and inactivation by H_2O_2 occurs, the non-destructive inhibition can be proposed as a safe storage of the biocatalyst via reducing the population of biocatalyst exposed the suicide substrate, since inhibited MP-11 does not undergo suicide inactivation (see Scheme 1).
(6) The introduced kinetic analysis based on the suicide-substrate inactivation of microperoxidase-11, can be used as a general model for studying the other similar bisubstrate peroxidase models in the presence of reversible inhibitors.

Excellent coincidence between experimental and calculated data based on the new integrated kinetic equation confirmed the accuracy of the model to obtain reliable apparent kinetic parameters for the simultaneous suicide-peroxide inactivation and competitive inhibition of microperoxidase-11 by the amino acids.

Acknowledgements

The financial support of the Iran National Science Foundation, research councils of Islamic Azad University and University of Tehran are gratefully acknowledged.

Appendix A

According to the mechanism shown in Scheme 1, the rate of depletion of enzyme due to the simultaneous inhibition and inactivation processes can be written as

$$\begin{aligned} -\frac{d[E]}{dt} &= k_3[CII][AH] + k_{-I}[E_I] - k_I[E] - k_1[E][H_2O_2] \\ &\quad + k_1[E][H_2O_2] - k_2[CI][AH] - k_i[CI][H_2O_2] \\ -\frac{d[E]}{dt} &= k_3[CII][AH] - k_{-I}[E_I] - k_I[E] - k_2[CI][AH] \\ &\quad -k_i[CI][H_2O_2] \end{aligned} \tag{A1}$$

Substitution of [CI] from equation (B3) and [CII] from Eq. (B5) in Appendix B gives:

$$\begin{aligned} -\frac{d[E]}{dt} &= k_3\left(\frac{k_1k_2[E]}{k_3k_i}\right)[AH] - k_{-I}[E_I] - k_I[E] \\ &\quad - k_2\left(\frac{k_1[E]}{(k_i)}\right)[AH] - k_i\left(\frac{k_1[E]}{(k_i)}\right)[H_2O_2] \\ -\frac{d[E]}{dt} &= -k_{-I}[E_I] - k_I[E] - k_2\left(\frac{k_1[E]}{k_i}\right)[AH] \\ &\quad -(k_1[E])[H_2O_2] \end{aligned} \tag{A2}$$

Using the rapid equilibrium approximation for the inhibited form of HRP, E_I, we have the following:

$$[E_I] = \frac{[E][I]}{K_I}, \qquad K_I = \frac{k_{-I}}{k_I}, \qquad [E_I] = \frac{[E][I]k_I}{k_{-I}} \tag{A3}$$

Substitution of $[E_I]$ from Eq. (A3) into Eq. (A2) gives:

$$\frac{-d[E]}{dt} = \frac{k_{-I}[E][I]k_I}{k_{-I}} - k_I[E] - (k_1[E])[H_2O_2] \tag{A4}$$

$$\frac{-d[E]}{dt} = k_I[E][I] - k_I[E] - k_1[E][H_2O_2] \tag{A5}$$

$$\frac{-d[E]}{dt} = \left\{k_I[I] - k_I - k_1[H_2O_2]\right\}[E] \tag{A6}$$

From Eq. (B10) in Appendix B we have the following:

$$\begin{aligned} \alpha = 2\left(\frac{k_1k_2}{k_i}\right)[E] \Rightarrow [E] = \frac{\alpha}{2k_1k_2/k_i} \Rightarrow \frac{-d[E]}{dt} = \frac{-1}{2k_1k_2/k_i}\left(\frac{d\alpha}{dt}\right) \\ = -\left(\frac{k_i}{2k_1k_2}\right) \times \left(\frac{d\alpha}{dt}\right) \end{aligned} \tag{A7}$$

Substitution into Eq. (A6):

$$\begin{aligned} -\left(\frac{k_i}{2k_1k_2}\right) \times \left(\frac{d\alpha}{dt}\right) &= \left\{k_I[I] - k_I - k_1[H_2O_2]\right\}[E] \\ &= \left\{k_I[I] - k_I - k_1[H_2O_2]\right\}\left[\frac{\alpha}{(2k_1k_2/k_i)}\right] \end{aligned} \tag{A8}$$

$$\frac{-d\alpha}{dt} = \left\{k_I[I] - k_I - k_1[H_2O_2]\right\}\alpha \tag{A9}$$

$$\left\{k_I[I] - k_I - k_1[H_2O_2]\right\}\alpha = (k_i^{app} + k_I^{app})\alpha \tag{A10}$$

$$k_{iI}^{app} = \left\{k_I[I] - k_I - k_1[H_2O_2]\right\} \tag{A11}$$

$$k_i^{app} = (k_1[H_2O_2]), \qquad k_I^{app} = k_I[I] - k_I \tag{A12}$$

Appendix B

Total concentration of HRP can be written as

$$[E]_{tot} = [E] + [E_I] + [C_I] + [C_{II}] + [E_i] \tag{B1}$$

E is the free enzyme at the resting state. Using the steady-state approximation for the enzyme kinetic intermediates in Scheme 1, we have the following:

$$\frac{d[C_I]}{dt} = (k_1[E] \times [H_2O_2]) - (k_i[C_I][H_2O_2]) \tag{B2}$$

$$\frac{d[C_I]}{dt} = 0 \Rightarrow [C_I] = \left(\frac{k_1[E]}{(k_i)}\right) \tag{B3}$$

$$\frac{d[C_{II}]}{dt} = (k_2[C_I] \times [AH]) - (k_3[C_{II}] \times [AH]) \tag{B4}$$

$$\begin{aligned} \frac{d[C_{II}]}{dt} = 0 \Rightarrow \left(k_2\left(\frac{k_1[E]}{k_i}\right)[AH]\right) - (k_3[C_{II}] \times [AH]) = 0 \\ [C_{II}] = k_2\left(\frac{k_1[E]}{(k_i)/k_3}\right) = \left(\frac{k_1k_2[E]}{k_3k_i}\right) \end{aligned} \tag{B5}$$

The rate of depletion of AH is (see Scheme 1):

$$\frac{-d[AH]}{dt} = (k_2[CI] \times [AH]) + (k_3[CII] \times [AH]) \tag{B6}$$

$$\begin{aligned} \frac{-d[AH]}{dt} &= \left\{k_2\left(\frac{k_1[E]}{k_i}\right)[AH]\right\} + \left\{k_3\left(\frac{k_1k_2[E]}{k_3k_i}\right)[AH]\right\} \\ \frac{-d[AH]}{dt} &= \left\{k_2\left(\frac{k_1[E]}{k_i}\right)[AH]\right\} + \left\{\left(\frac{k_1k_2[E]}{k_i}\right)[AH]\right\} \end{aligned} \tag{B7}$$

$$\begin{aligned} \frac{-d[AH]}{dt} &= \left\{k_2\left(\frac{k_1}{k_i}\right) + \left(\frac{k_1k_2}{k_i}\right)\right\}[E] \times [AH] \\ \frac{-d[AH]}{dt} &= \left\{k_2\left(\frac{k_1}{k_i}\right) + \left(\frac{k_1k_2}{k_i}\right)\right\}[E] \times [AH] \end{aligned} \tag{B8}$$

$$\frac{-d[AH]}{dt} = 2\left(\frac{k_1k_2}{k_i}\right)[E][AH] \tag{B9}$$

$$\alpha = 2\left(\frac{k_1k_2}{k_i}\right)[E] \tag{B10}$$

References

[1] W.J. Chuang, Y.D. Chang, W.Y. Jeng, J. Inorg. Biochem. 75 (1999) 93–97.
[2] N. Feder, J. Cell Biol. 51 (1971) 339–343.
[3] C. Veeger, J. Inorg. Biochem. 91 (2002) 35–45.
[4] W. Huang, Z. Zhang, X. Han, J. Tang, Z. Peng, S. Dong, E. Wang, Biophys. Chem. 94 (2001) 165–173.
[5] K.J. Reszka, Y. O'Malley, M.L. Mccormick, G.M. Denning, B.E. Britigan, Free Radic. Biol. Med. 36 (11) (2004) 1448–1459.
[6] M. Oyadomari, M. Kabuto, H. Wariishi, H. Tanaka, Biochem. Eng. J. 15 (2003) 159–164.
[7] K.J. Reszka, M.L. Mccormick, B.E. Britigan, Free Radic. Biol. Med. 35 (1) (2003) 78–93.
[8] L.N. Grinberg, P.J. O'Brien, Z. Hrkal, Free Radic. Biol. Med. 26 (1999) 214–219.
[9] Z.X. Guo, H.X. Shen, L. Li, Mikrochim. Acta (1999) 131.
[10] H.R. Kalish, L. Latos-Grazynski, A.L. Balch, J. Am. Chem. Soc. 122 (2000) 12478–12486.
[11] S.B. Brown, T.C. Dean, P. Jones, M.L. Kremer, Trans. Faraday Soc. 66 (1970) 1485–1490.
[12] E.S. Ryabova, P. Rydberg, M. Kolberg, E. Harbitz, A.L. Barra, U. Ryde, K.K. Andersson, E. Nordlander, J. Inorg. Biochem. 99 (3) (2005) 852–863.
[13] T.G. Traylor, W.A. Lee, D.V. Stynes, J. Am. Chem. Soc. 106 (1984) 755–764.
[14] Y. Reyes-Ortega, C. Alvarez-Toledano, D. Ramirez-Rosales, A. Sanchez-Sandoval, E. Gonzalez-Vergara, R. Zamorano-Ulloa, J. Chem. Soc., Dalton Trans. (1998) 667–674.
[15] T.L. Poulos, J. Biol. Inorg. Chem. 1 (1996) 356–359.
[16] D.B. Goodin, J. Biol. Inorg. Chem. 1 (1996) 360–363.
[17] S.I. Ozaki, M.P. Roach, T. Matsui, Y. Watanabe, Acc. Chem. Res. 34 (2001) 818–825.
[18] J.A. Laszlo, D.L. Compton, J. Mol. Catal. B 18 (2002) 109–120.
[19] J.S. Wang, H.K. Baek, H.E. Van Wart, Biochem. Biophys. Res. Commun. 179 (3) (1991) 1320–1324.
[20] D.A. Baldwin, H.M. Marques, J.M. Pratt, J. Inorg. Biochem. 30 (3) (1987) 203–2175.
[21] S.G. Waley, Biochem. J. 227 (3) (1985) 843–849.
[22] S.G. Waley, Biochem. J. 185 (3) (1980) 771–773.
[23] S.G. Waley, Biochem. J. 279 (1) (1991) 87–94.
[24] S. Longu, A. Mura, A. Padiglia, R. Medda, G. Floris, Phytochemistry 66 (2005) 1751–1758.
[25] M. Ghadermarzi, A.A. Moosavi-Movahedi, Ital. J. Biochem. 46 (4) (1997) 197–205.

[26] A.A. Moosavi-Movahedi, K. Nazari, M. Ghadermarzi, Ital. J. Biochem. 48 (1) (1999) 9–17.
[27] M. Khosraneh, A. Mahmoudi, H. Rahimi, K. Nazari, A.A. Moosavi-Movahedi, J. Enzyme Inhib. Med. Chem. 22 (6) (2007) 677–684.
[28] K. Nazari, N. Esmaeili, A. Mahmoudi, H. Rahimi, A.A. Moosavi-Movahedi, Enzyme Microb. Technol. 41 (2007) 226–233.
[29] B. Valderrama, M. Ayala, R. Vazquez-Duhalt, Chem. Biol. 9 (2002) 555–565.
[30] S. Okazaki, S. Nagasawa, M. Goto, S. Furusaki, H. Wariishi, H. Tanaka, Biochem. Eng. J. 12 (2002) 237–241.
[31] F. Anjum, V. Rishi, F. Ahmad, Biochim. Biophys. Acta 1476 (1) (2000) 75–84.
[32] S. Taneja, F. Ahmad, Biochem. J. 303 (1) (1994) 147–153.
[33] V. Rishi, F. Anjum, F. Ahmad, W. Pfeil, Biochem. J. 329 (1998) 137–141.
[34] R.E.C. Bardsley, G. William, Biochem. J. 145 (1975) 93–103.
[35] K. Nazari, A. Mahmoudi, M. Shahrooz, R. Khodafarin, A.A. Moosavi-Movahedi, J. Enzyme Inhib. Med. Chem. 20 (3) (2005) 285–292.
[36] L. Casella, L.D. Gioia, G.F. Silvestri, E. Monzani, C. Redaelli, R. Roncone, L. Santagostini, J. Inorg. Biochem. 79 (2000) 31–39.
[37] R. Nakajima, I. Yamazaki, J. Biol. Chem. 262 (1987) 2576–2581.
[38] A. Mazmudar, S. Adak, R. Chatterjee, K. Banerjee, Biochem. J. 324 (1997) 713–719.
[39] R.W. Noble, Q.H. Gibson, J. Biol. Chem. 245 (1970) 2409–2413.
[40] R. Yousefi, A.A. Saboury, M. Ghadermarzi, A.A. Moosavi-Movahedi, Bull. Korean Chem. Soc. 21 (6) (2000) 567–570.
[41] M.A. Ator, K. Shantha, P.R. Ortiz de Montellano, J. Biol. Chem. 262 (1987) 14954–14960.
[42] I. Yamazaki, R. Nakajima, in: H. Greppin, C. Penel, T. Gaspar (Eds.), Molecular and Physiological Aspects of Plant Peroxidases, University of Geneva, Geneva, Switzerland, 1992, pp. 71–84.
[43] Y. Hayashi, I. Yamazaki, J. Biol. Chem. 254 (1979) 9101–9106.
[44] A. Mahmoudi, K. Nazari, M. Khosraneh, A.A. Moosavi-Movahedi, Enz. Microb. Technol., in press.
[45] H.B. Dunford, J.S. Stillman, Coord. Chem. Rev. 19 (1976) 187–251.
[46] K. Nazari, A. Mahmoudi, R. Khodafarin, A.A. Moosavi-Movahedi, A. Mohebi, J. Ir. Chem. Soc. 2 (3) (2005) 232–237.
[47] F.M. Veronese, M. Morpurgo, Bioconjugation Pharm. Chem. IL Farmaco 54 (1999) 497–516.
[48] R.M. Roat-Malone, Bioinorganic Chemistry, John Wiley & Sons, 2002, pp. 25–33 (INC Pub).
[49] A. Schejter, A. Lanir, N. Epstein, Arch. Biochem. Biophys. 174 (1976) 36–44.
[50] A.A. Moosavi-Movahedi, A.R. Golchin, K. Nazari, J. Chamani, A.A. Saboury, S.Z. Bathaie, S. Tangestani-Nejad, Thermochim. Acta 414 (2004) 233–241.
[51] B. Farzami, K. Nazari, A.A. Moosavi-Movahedi, J. Sci. I.R. Iran 8 (1997) 209–216.
[52] K. Nazari, S. Shokrollahzadeh, A. Mahmoudi, F. Mesbahi, N. Seyed-Matin, A.A. Moosavi-Movahedi, J. Mol. Catal. A 239 (2005) 1–9.
[53] T. Palmer, Understanding Enzymes, 3rd ed., Ellis Harwood Pub, Sussex, 1991, pp. 139–146.
[54] Q. Guo, C.D. Detweiler, R.P. Mason, J. Biol. Chem. 279 (13) (2004) 13272–13283.